IBRACON Structures and Materials Journal
Revista IBRACON de Estruturas e Materiais
ISSN 1983-4195 ismj.org

ORIGINAL ARTICLE

Proposal for estimating the punching shear load-carrying capacity of steel fibers reinforced concrete flat slabs

Proposta para estimativa de capacidade de carga na punção de lajes lisas de concreto armado reforçado com fibras de aço

Lucas Guedes Dantas[a]
Leonardo Henrique Borges de Oliveira[b]
Antônio Carlos dos Santos[a]
Leandro Mouta Trautwein[c]

[a]Universidade Federal de Uberlândia – UFU, Faculdade de Engenharia Civil, Uberlândia, MG, Brasil
[b]Universidade Federal Rural do Semi-Árido – UFERSA, Departamento de Engenharia e Tecnologia, Pau dos Ferros, RN, Brasil
[c]Universidade Estadual de Campinas – UNICAMP, Faculdade de Engenharia Civil, Arquitetura e Urbanismo, Campinas, SP, Brasil

Received 16 December 2021
Accepted 17 December 2022

Abstract: This paper proposes an adjusted function for estimating the punching shear load-carrying capacity of concrete flat slabs without shear reinforcement according to the Brazilian standard code. The Adjusted function considers the influence of the steel fiber content. Data from 68 steel fiber reinforced concrete slabs (SFRC slabs) were used, simulating the connection of flat slabs with square section columns. These slabs were obtained from a study conducted by 14 different researchers. The parameters used for the adjusted function were the fiber content and the compressive strength of the concrete. The adjusted function was obtained by curve-fitting. The result from the adjusted function shows a relation in the order of 1.3 between the experimental rupture load and the calculated load, a value close to that already obtained by the normative text when the calculation is for conventional concrete. This shows that the proposal presented here keeps the same level of security with a confidence index of 96% in comparison with other authors' models presented in this study.

Keywords: load-carrying capacity, steel fiber reinforced concrete, SFRC, punching shear, flat slabs.

Resumo: Este trabalho propõe uma função para estimar a capacidade de carga com ruptura na punção de lajes lisas de concreto sem armadura de cisalhamento de acordo com a norma brasileira. A função considera a influência do teor de fibra de aço na adição do concreto. Foram utilizados dados de 68 lajes de concreto armado com fibras de aço, simulando a ligação de lajes lisas com pilares de seção quadrada. Essas lajes foram obtidas a partir de um estudo realizado por 14 pesquisadores diferentes. Os parâmetros utilizados para a função foram o teor de fibras e a resistência à compressão do concreto. A função foi obtida por ajuste de curva. O resultado da função ajustada mostra uma relação da ordem de 1,3 entre a carga de ruptura experimental e a carga calculada, valor próximo ao já obtido pelo texto normativo quando o cálculo é para concreto convencional. Isso mostra que a proposta aqui apresentada mantém o mesmo nível de segurança com um índice de confiança de 96% em comparação com os modelos de outros autores apresentados neste estudo.

Palavras-chave: capacidade de carga, concreto armado reforçado com fibras de aço, CRF, punção, lajes lisas.

How to cite: L. G. Dantas, L. H. B. Oliveira, A. C. Santos, and L. M. Trautwein, "Proposal for estimating the punching shear load-carrying capacity of steel fibers reinforced concrete flat slabs," *Rev. IBRACON Estrut. Mater.*, vol. 16, no. 5, e16509, 2023, https://doi.org/10.1590/S1983-41952023000500009

Corresponding author: Leonardo Henrique Borges de Oliveira. E-mail: leonardo.oliveira@ufersa.edu.br
Financial support: Coordenação de Aperfeiçoamento de Pessoal de Nível Superior (CAPES).
Conflict of interest: Nothing to declare.
Data Availability: The data that support the findings of this study are available from the corresponding author, Leonardo Henrique Borges de Oliveira, upon reasonable request.

1 INTRODUCTION

The traditional structural system of reinforced concrete structures is characterized by slabs, beams and columns. In this system, loads are applied directly to the slabs, which transfers it to the beams. The beams transfer the efforts to the columns, which are supported by the foundation of the building. However, a new system emerged at the beginning of the 20th century, as an innovative structural model, to which beams are not used and the forces from the slabs are directly transferred to the columns. Because the slabs have uniformity due to the absence of the beams, they were called flat slabs Gasparini [1]. However, in this structural system there is the possibility of collapsing the flat slabs by punching shear mechanism.

Punching Shear can occur as the result of a concentrated load applied to a structural element. In flat slabs, for example, the collapse occurs in the connection with structural elements. The magnitude of shear efforts generated by the concentrated forces are high, which can cause the rupture of the slab.

One of the punching shear load carrying-capacity design methods adopted by several standards codes is called the critical perimeter surface. It consists of verifying whether a uniform shear stress that is applied to a determined critical surface, perpendicular to the slab's median plane, located at a distance from the face of the column is compatible with the concrete's shear strength in this same region. If the shear strength is not sufficient to withstand the shear stress, the use of punching shear reinforcement is indicated. ABNT NBR 6118 (2014) [2] indicates studs-type connectors preferably as a punching shear reinforcement.

According to ABNT NBR 6118 (2014) [2], the shear stress is given by :

$$\tau_{Sd} = \frac{F_{Sd}}{ud} \tag{1}$$

Where:
F_{Sd} = Load-carrying capacity (Force);
u = shear critical perimeter (Length);
d = average slab effective depth in both directions (Length).

For slabs without punching shear reinforcement, the stress of the compressive concrete diagonal is checked, considering the critical perimeter as the perimeter of the column or loaded area. In addition, a control perimeter with a slab distant up to twice the average of the slab's effective depth (d) is checked. Figure 1 shows the control perimeter for central columns sections of rectangular and circular sections .

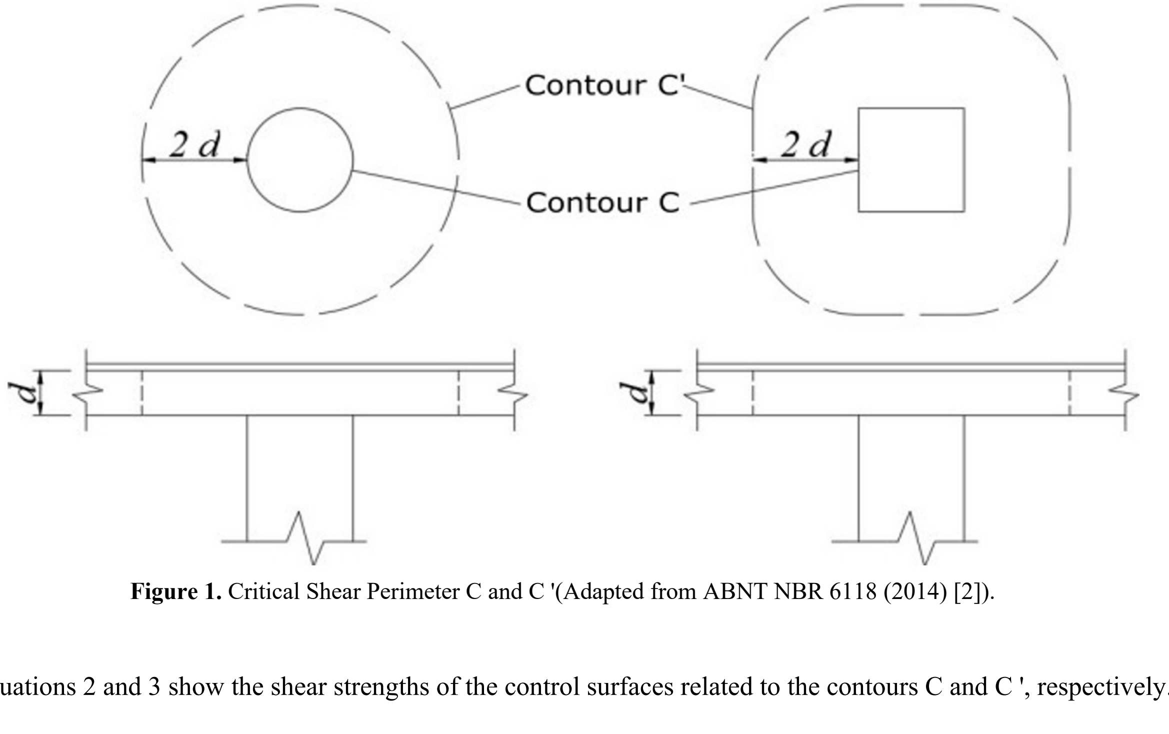

Figure 1. Critical Shear Perimeter C and C '(Adapted from ABNT NBR 6118 (2014) [2]).

Equations 2 and 3 show the shear strengths of the control surfaces related to the contours C and C ', respectively.

$$\tau_{rd1} = 0.27(1 - \frac{f_{ck}}{250})f_{cd} \tag{2}$$

$$\tau_{rd2} = 0.13\left(1 + \sqrt{\frac{20}{d}}\right)(100\rho f_{ck})^{1/3} \tag{3}$$

Where:
τ_{rd1}, τ_{rd2} = shear strength of slabs without punching reinforcement (MPa);
f_{ck} = concrete's compressive strength;
f_{cd} = (f_{ck}/γ_c) – concrete design strength;
d = Average slab effective depth in both directions;
$\rho = (\rho_x\rho_y)^{0.5}$ – Flexural Reinforcement Ratio in both directions of the slab, at up to 3d from the edge of the column or loaded area (dimensionless).

The estimated load-carrying capacity of slabs can be found by replacing τ_{rd1} or τ_{rd2} in Equation 1 and isolating the calculation force, as shown in Equation 4:

$$F_{rd} \leq \begin{cases} \tau_{rd1}ud \\ \tau_{rd2}ud \end{cases} \tag{4}$$

The accuracy of the standard code equations in comparison to experimental results presents a significant discrepancy. According to Dantas [3], who compares a series of experimental results of slabs without shear reinforcement, on average the relationship between the experimental load-carrying capacity and one obtained according to ABNT NBR 6118 (2014) [2] is 1.3. It is important to note that this relationship is obtained without the use of normative safety factors of increase / reduction.

In general, the addition of steel fibers to the referred mechanism contributes to the ductility of the system, cracking control and load redistribution [4]–[10]]. Also, experimental tests showed that monitored reinforcement bars presented a reduction in the strains observed in comparison to concrete slabs without steel fibers [8]. Other authors presented that the critical shear perimeter presented an increase by the addition of steel fiber content ([4] and [11]]). This differences in performance contribute to increasing the load-carrying capacity of flat slabs.

Recently, it was published a Brazilian Standard Code for designing fiber reinforced concrete elements, the ABNT NBR 16935 (2021) [12]]. The Brazilian code recommendations for punching shear depends on post-cracking parameters $f_{Ftu,k}$, demanding a $P \times CMOD$ from a three-point bending test. This study presents an alternative study for estimating the load-carrying capacity for steel fibers reinforced concrete flat slab collapsing by punching based on the results from 68 experimental tests and without the need for post-cracking parameters.

Regarding design, recent research has shown that the use of steel fibers can increase the punching shear strength of flat slabs, as well as transform the dynamics of the rupture of the slab-column connection, from fragile to ductile [4]–[6], [13]–[23]. The models studied in this paper presented this increase compared to other to slabs molded by conventional concrete.

This work aims to propose an adjusted function in the formulation existing in the NBR 6118 standard code ABNT NBR 6118 (2014) [2] that estimates the load-carrying of flat reinforced concrete slabs, considering the steel fibers contents. To determine this adjustment function, results from 68 tests of fiber reinforced concrete slabs supported on their edges and tested under concentrated load applied in a square section, using the slab-column connection (without the use of shear reinforcement).

2 ANALYTICAL METHOD

The proposed adjustment Function G is based on two parameters. The first parameter is given by the steel fiber content. The second is the dimensionless parameter k, which is adjusted according to the experimental results and defined according to the concrete compressive strength (f_c). The adjustment function applied to the NBR 6118 standard equation ABNT NBR 6118 (2014) [2] is given by (5) and (6):

$$\tau_{rd1} = 0.27\left(1 - \frac{f_{ck}}{250}\right)f_{cd}G(V_f, k) \tag{5}$$

$$\tau_{rd2} = 0.13\left(1+\sqrt{\frac{20}{d}}\right)(100\rho f_{ck})^{1/3}G(V_f,k) \tag{6}$$

Since τ_{rd2} is lower than τ_{rd1} in most cases, adjustment of the dimensionless parameter k is performed only in Equation 6. Still, according to Dantas [3], several types of adjusted function are proposed for the Function G, of which, the one with the best adaptability in relation to the experimental results is given by Equation 7.

$$G(V_f,k) = (1+ln\left(1+kV_f\right)) \tag{7}$$

Where:
k = Parameter that correlates the compressive strength of concrete (dimensionless);
V_f = Steel fiber content (% by volume of concrete).

2.1 Definition of the Parameter k

The function G was adjusted by a logarithmic fitting-curve of the experimental tests conducted by authors presented in a database. Table 1 shows the list of researchers and the number of tests used to adjust the proposed function. All experimental tests from this study database simulate the slab-column connection, with square section columns molded in reinforced concrete and SFRC slabs without shear reinforcement.

The parameter k is adjusted according to the compressive strength of the concrete (Table 2). The method used to adjust the parameter is based on two hypotheses: the average of the experimental / theoretical rupture load ratio is the closest to one (1); in none of the individual results, the experimental / theoretical rupture load ratio is less than one (1). Table 2 shows each compressive strength used. Figure 2 shows the iterative process to obtain the parameter k.

Table 1. Experimental papers

Author	Tests	Author	Tests
Narayanan and Darwish [4]	12	Musse [19]	2
Theodorakopoulos and Swamy [13]	20	De Hanai and and Holanda [20]	8
Shaaban and Gesund [14]	12	Cheng and Parra-Montesinos [21]	10
Harajli et al. [15]	10	Nguyen-Minh et al. [22]	12
Vargas [16]	6	Gouveia et al. [23]	6
Azevedo [17]	6	Barros et al. [5]	8
McHarg et al. [18]	4	Alves [6]	3

The process of adjusting the Parameter k consists of an iterative method where the Equation 4 to 7 are applied from each result of the experimental test of the data base varying k. The steel fibers behavior is sensitive to the concrete compressive strength, which indirectly influences the bond mechanism of the fiber in the concrete matrix. Thus, the Parameter k from the Function G is adjusted for each compressive strength values of the database experimental tests (see Figure 2). Parameter k is defined by minimizing an Error Parameter of subsequent iterations(R_i and R_{i-1}, where i is the iteration number, see Figure 2).

Table 2. Analysis intervals of parameter k.

Concrete strength (MPa)	Parameter
20~30	k_{20}
30~40	k_{30}
40~50	k_{40}
50~60	k_{50}
60~70	k_{60}
70~80	k_{70}
80~90	k_{80}

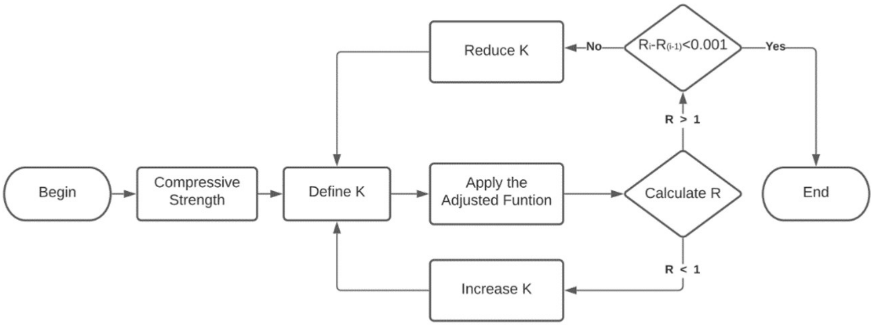

Figure 2. Flowchart of the iterative process .

The parameters used in the proposed adjustment function are the concrete compressive strength (f_c), flexural reinforcement ratio (ρ), slab effective depth (correlated with slab thickness, h), equivalent square column width (b_p), steel fiber content in percentage of the concrete volume (V_f).

From the pre-selected data, the experimental results of some researchers are discarded for the determination of parameter k. This assumption is because the relation of the experimental load capacity (P_{exp}) and the load-carrying capacity estimated by ABNT NBR 6118 (2014) [2] (P_{NBR}) of the slabs reference values are outside the "appropriate safety" range according to Collins [24], Dantas [3]. Still, in the whole process of the analytical model, despite being based on the equations of ABNT NBR 6118 (2014) [2], the load increase and / or resistance reduction coefficients of that standard are not used. In total, there are 90 slabs, 22 of which are reference slabs.

3 RESULTS AND DISCUSSIONS

Figure 3 show the dispersion of h, f_c, ρ, b_p, and V_f, of the 68 slabs to adjust the parameter k.

From the results of the adjusting process showed in Figure 2, Table 3 shows the average results of the relationship ($R_{e,tm}$) experimental load-carrying capacity (P_{exp}) and theoretical load-carrying capacity of the model (P_{mod}). In addition, Table 4 presents the results of the Parameter k for each compressive strength range.

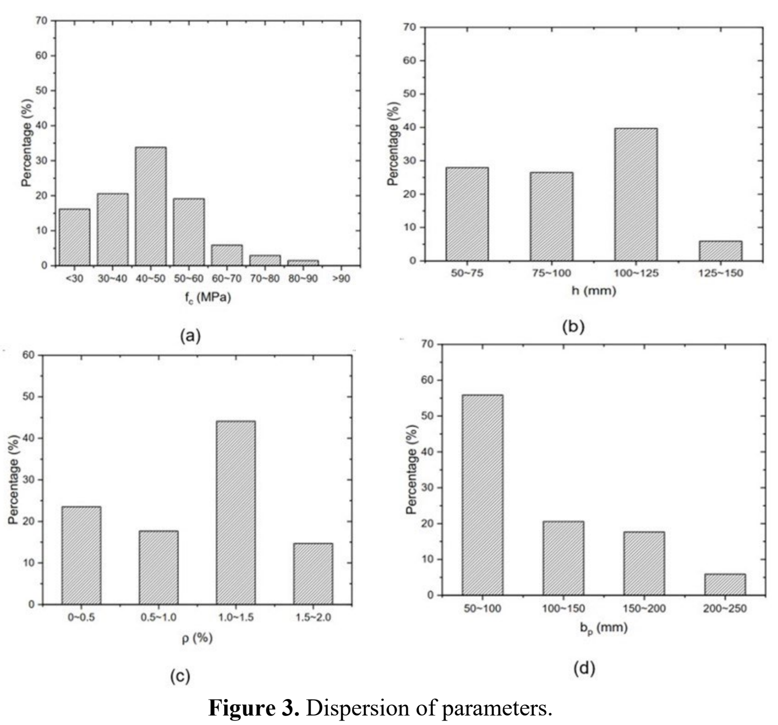

Figure 3. Dispersion of parameters.

The adjusted ABNT NBR 6118 (2014) [2] equations are presented in Equations 8 to 10:

$$F_{rd} = Minimum(\tau_{rd1}, \tau_{rd2})ud \tag{8}$$

$$\tau_{rd1} = 0.27(1 - \frac{f_c}{250})f_c[1 + ln\left(1 + kV_f\right)] \tag{9}$$

$$\tau_{rd2} = 0.13\left(1 + \sqrt{\frac{20}{d}}\right)(100\rho f_c)^{\frac{1}{3}}[1 + ln\left(1 + kV_f\right)] \tag{10}$$

Where:
k = Dimensionless parameter, defined by the strength class of the concrete (Table 4);
V_f = Steel fiber content in % of m^3 volume of concrete.

Table 3. Experimental / theoretical rupture load ratio by strength class.

f_c (MPa)	Number of slabs	k	$R_{e,m}$		
			X	***S***	***CV***
20~30	10	0.248	1.118	0.171	15.32
30~40	15	0.132	1.262	0.167	13.21
40~50	23	0.208	1.305	0.201	15.39
50~60	13	0.319	1.11	0.082	7.37
60~70	4	0.548	1.031	0.027	2.61
70~80	2	0.615	1.019	0.026	2.6
80~90	1	0.218	1	-	-
Total	68	-	1.199	0.187	15.59

$R_{e,m}$ – Relationship between the experimental and proposed load-carrying capacity load; X – Sample mean; S – Sample standard deviation; CV – Coefficient of variation in %.

The experimental results include only connections of center and square section slabs and columns. Therefore, this adjusted function is recommended to be applied in similar situations. There is a relatively small number of tests that fit to compressive strength above 60 MPa, which prevent the definition of a Parameter k for this range that is statistically satisfactory.

Although the analysis of the fibers is done according to the fiber content (in percentage), factors such as fiber strength and fiber geometry also affect the behavior of the SFRC, but not as significantly, compared to the fiber content Narayanan and Darwish [4] De Hanai and Holanda [20]. Figure 4 presents the results of the relation between the experimental load-carrying capacity and proposed adjusted function (R_{em}) according to the concrete compressive strength applied on each experimental tests from database.

Table 4. Parameter k.

Compressive Strength (f_c)	Parameter	Value
20~30	k_{20}	0.248
30~40	k_{30}	0.132
40~50	k_{40}	0.208
50~60	k_{50}	0.319
60~70	k_{60}	0.548
70~80	k_{70}	0.615
80~90	k_{80}	0.218

The results of $R_{e,m}$ showed that the proposed adjusted function presented a conservative estimative of the load-carrying capacity of experimental tests for all compressive strength from the studied experimental test of the database. In other words, all values of $R_{e,m}$ are higher than 1.0 which means that the load-carrying capacity estimated by the proposed adjusted function is lower than the experimental tests from the authors of the data base. Compressive strength in a range of 30-40MPa present the most conservative estimative while compressive strength in a range of 60-70MPa present $R_{e,m}$ less conservative in comparison with other results from Figure 4.

A comparative study of the load-carrying capacity of the experimental tests from data base and other analytical and theoretical model proposed by Narayanan and Darwish [4], Harajli et al. [15], De Hanai and Holanda [20] and Higashiyama et al. [11] is showed in Figure 5. A comparative estimative from the proposed model presented in this paper is also presented in Figure 5a. For each graph in Figure 5, the x-axis presents the load-carrying capacity measured on the experimental tests, the y-axis presents the load-carrying capacity estimated by the respective theoretical model and each point of the graph is an experimental test from the database. For an estimated load-carrying capacity equal to the measured on the experimental test the point should be projected in a 1:1 line. Points projected above the 1:1 line presents experimental results lower than the estimated results by the theoretical model. Points projected below the 1:1 line presents experimental results higher than estimated by the theoretical model (conservative results).

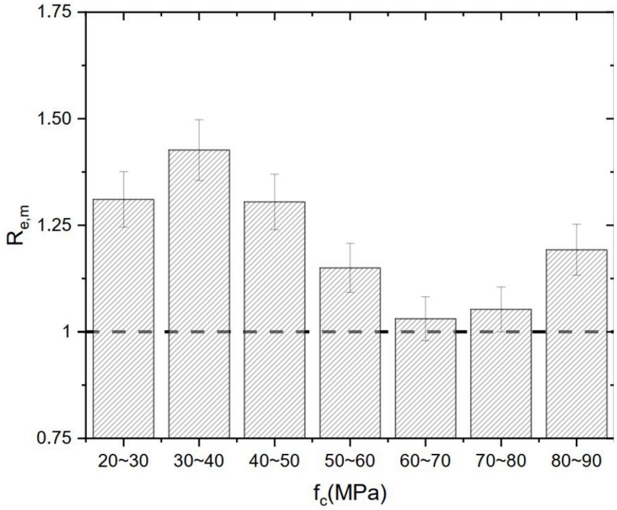

Figure 4. Average results of the application of the adjustment function in relation to f_c.

From Figure 5, the proposed model (Figure 5a) presents a lesser dispersion of the relationship between experimental and theoretical load-carrying capacity, especially for results up to 200 kN. The proposed model also presents a tendency to estimate the load carrying capacity of slabs that reach higher values (for example, 500kN). The dispersion of the projected point that represents the experimental tests from the data base is higher for the other authors estimative models, which means that the results were not accurate. In addition, some results are projected above the 1:1 line, which means that the load-carrying capacity measured on the experimental tests are lower that the estimated results, which presents a risky estimative. This could be observed in Figure 5b to 6e (Narayanan and Darwish [4], Harajli et al. [15], De Hanai and Holanda [20] and Higashiyama et al. [11], respectively).

Table 5. Confidence index.

Model	$R_{e,m}$ (Mean)	$R_{e,m}$ (Standard Deviation)	$R_{e,m}$ (Variation Coefficient)	Confidence Indicator
Proposed Model	1.29	0.23	18%	96%
Narayanan and Darwish [4]	1.59	0.76	48%	74%
Harajli et al. [15]	1.50	0.65	44%	74%
De Hanai and Holanda [20]	1.50	0.60	40%	77%
Higashiyama et al. [11]	1.49	0.56	37%	72%

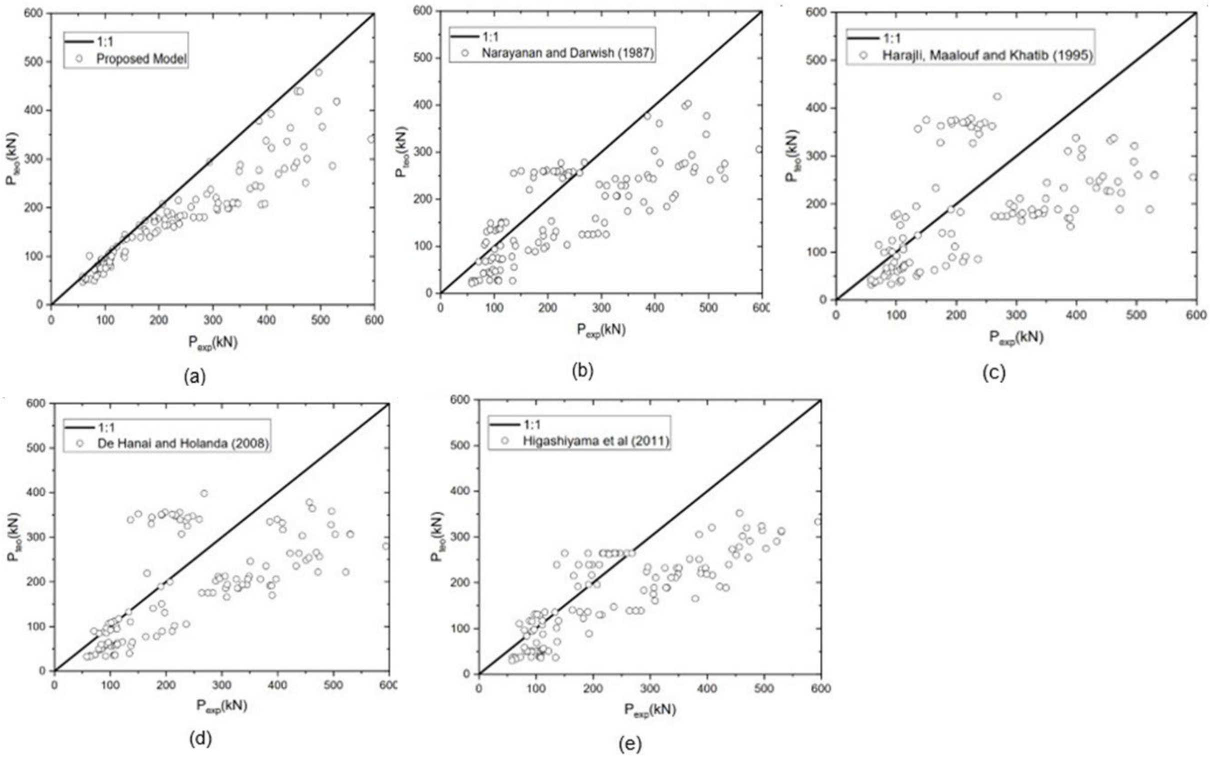

Figure 5. Comparison of rupture load prediction models.

Defining as a confidence index the percentage of slabs for which the experimental load is greater than the theoretical load, the proposed model presents a confidence indicator of 96%. The confidence indicator was calculated considering all slabs from database. However, the other models analyzed presented lower confidence indicators. In addition, the proposed model presents an average relationship between experimental and estimated results of 1.29 while Models proposed by other authors presents $R_{e,m}$ from 1.49 (Higashiyama et al. [11]) to 1.59 (Narayanan and Darwish [4]), this could be observed by the dispersion of the results on Figure 5. Table 5 shows the relationship of the confidence index.

Phenomena observed in steel fiber reinforced concrete are considered in Narayanan and Darwish [4], Harajli et al. [15] and Higashiyama et al. [11] models, for example, the change in the punching shear rupture surface due to the addition of steel fibers in the concrete mixture. However, the parameters in these models to considered are empirical values and could lead in to not accurate estimative.

4 COMPARISON WITH THE BRAZILIAN CODE ABNT NBR 16935 (2021) [12]

To compare the recommendations of ABNT NBR 16935 (2021) [12] and the proposed model in this paper, a case study of estimating the punching shear load-carrying capacity was conducted. Four flat slabs experimental tests conducted by Alves et al. [25] were estimated.

ABNT NBR 16935 (2021) [12] demands the post-cracking parameters, such as P x CMOD curve of steel fiber concrete. The study and production of the fiber and concrete materials proportion for these flat slabs experimental tests were conducted by Silva [26], which studied the P x CMOD curve of the same concrete used to mold the experimental tests of Alves et al. [25].

The experimental test was conducted in 1800mm x 1800mm x 130mm flat slabs, molded in steel fiber reinforced concrete with the addition of 50kg/m^3 ($v_f = 0.64\%$) of a hooked-end type DRAMIX RC 50/60. The fibers had a nominal diameter of 0.90 mm, a length of 60 mm and a size factor of 65. The experimental P x CMOD test was conducted in a 150mm x 150mm x 500mm concrete specimen with 125mm notch in its midspan. Table 6 presents the properties of the experimental tests conducted by Alves et al. [25]. Table 7 presents the properties of the steel fiber reinforced concrete properties of the experimental tests conducted by Silva [26]. For further details of the experimental tests the authors recommend reading study of Alves et al. [25] and Silva [26].

Table 6. Experimental tests properties from Alves et al. [25].

Slab	L	h	d	a	ρ	v_f	f_c	P_{exp}
	(mm)	(mm)	(mm)	(mm)		(%)	(MPa)	(kN)
L1-50-1	1800	130	99	250	0.016	0.64	42.01	469
L1-50-2	1800	130	99	250	0.016	0.64	42.01	469
L2-50	1800	130	98	250	0.016	0.64	42.01	513
L3-50	1800	130	99	250	0.016	0.64	42.01	455

L – Slab length; h – Slab thickness; d – Average effective depth measured after the experimental tests; a – Column length; ρ – Flexural reinforcement ratio; v_f – Steel fiber content; f_c – Average concrete compressive strength; P_{exp} – Punching shear load-carrying capacity measured in the test;

Table 7. Steel fibers reinforced concrete P x CMOD properties from Silva [26]

Identification	$CMOD$	Opening	$F_{R,i}$	$f_{R,i}$
		(mm)	(kN)	(MPa)
C40/50-1	$CMOD_1$	0.5	13.24	4.24
	$CMOD_2$	1.5	12.89	4.12
	$CMOD_3$	2.5	12.67	4.06
	$CMOD_4$	3.5	11.05	3.54
C40/50-2	$CMOD_1$	0.5	12.83	4.10
	$CMOD_2$	1.5	13.21	4.23
	$CMOD_3$	2.5	11.79	3.77
	$CMOD_4$	3.5	11.90	3.81

$CMOD_i$ – Crack mouth opening displacement for the i opening displacemnet; $F_{R,i}$ – Residual force measured at $CMOD_i$; $f_{R,i}$ – Residual tensile strength measured at $CMOD_i$;

From Table 6 and Tabel 7, L1-50-1 and L2-50 were molded with C40/50-1 and L1-50-2, L3-50 were molded with C40/50-2, the average compressive strength for both specimens was 42MPa. The load-carrying capacity estimate model by the recommendation of ABNT NBR 16935 (2021) [12] is presented in Equation 11 to 14.

$$V_{Rd} = V_{Rd,F} + V_{Rd,s} \tag{11}$$

$$V_{rd,F} = V_{Rd,f} + V_c \tag{12}$$

$$V_{Rd,f} = \frac{f_{Ftu,k}}{\gamma_F} \mu d \tag{13}$$

$$f_{Ftu,k} = \frac{f_{R3}}{3} \tag{14}$$

Where V_{Rd} is the load-carrying capacity, $V_{Rd,F}$ is the contribution of the steel fiber reinforced concrete, $V_{Rd,s}$ is the contribution of the shear reinforcement ratio, $V_{Rd,f}$ is the fiber contribution in the load carrying capacity of the steel fiber reinforced concrete, V_c is the contribution of the concrete in the load carrying capacity of the steel fiber reinforced concrete, $f_{Ftu,k}$ is the tensile residual strength of the steel fiber reinforced concrete, μ is the critical punching shear perimeter, d is the effective depth and f_{R3} is the residual tensile strength measured at $CMOD_3$.

Table 8 presents the results from the comparison of the estimative of the load-carrying capacity conducted by ABNT NBR 16935 (2021) [12]. Table 9 presents the results from the Proposed Model. Table 10 presents the comparison of the ABNT NBR 16935 (2021) [12] and the Proposed Model.

Table 8. Estimative of the load-carrying capacity – ABNT NBR 16935 (2021) [12]

Slab	d (mm)	ρ	f_c (MPa)	f_{R3} (MPa)	$f_{Ftu,k}$ (MPa)	τ_{Rd1} (MPa)	μ (mm)	V_c (kN)	$V_{Rd,f}$ (kN)	$V_{Rd,ABNT}$ (kN)
L1-50-1	99	0.016	42	4.06	1.35	1.77	2244.07	393.66	300.32	693.98
L1-50-2	99	0.016	42	3.77	1.26	1.77	2244.07	393.66	279.32	672.98
L2-50	98	0.016	42	4.06	1.35	1.77	2231.50	393.66	295.62	684.28
L3-50	99	0.016	42	3.77	1.26	1.77	2231.50	393.66	274.95	663.61

Table 9. Estimative of the load-carrying capacity – Proposed model

Slab	D (mm)	ρ	f_c (MPa)	v_f (%)	V_c (kN)	k	$V_{Rd,Prop}$ (kN)
L1-50-1	99	0.016	42	0.64	393.66	0.208	442.86
L1-50-2	99	0.016	42	0.64	393.66	0.208	442.86
L2-50	98	0.016	42	0.64	393.66	0.208	437.23
L3-50	99	0.016	42	0.64	393.66	0.208	437.23

Table 10. Comparison Experimental, ABNT NBR 16935 (2021) [12] and Proposed Model

Slab	$V_{Rd,ABNT}$ (kN)	$V_{Rd,Prop}$ (kN)	V_{exp} (kN)	$V_{Rd,ABNT}/V_{Rd,Prop}$	$V_{exp}/V_{Rd,ABNT}$	$V_{exp}/V_{Rd,Prop}$
L1-50-1	693.98	442.86	469	1.57	0.68	1.06
L1-50-2	672.98	442.86	469	1.52	0.70	1.06
L2-50	684.28	437.23	513	1.57	0.75	1.17
L3-50	663.61	437.23	455	1.52	0.69	1.04

Since there were no shear reinforcement in Alves et al. [25] experimental tests, $V_{rd,s}$ was assumed as zero. As a simplification, ABNT NBR 16935 (2021) [12] recommend calculate the V_c with the same recommendation for conventional concrete presented in ABNT NBR 6118 (2014) [2]. f_{R3} was obtained by the P x CMOD curves conducted by Silva [26] and presented in Table 7. In addition, the safety factors were assumed as 1, including γ_F presented in Equation 13. This decision was assumed to compare the results of the proposed method and the ABNT 16935 (2021) [12] without any interference of safety factors. The Equation 4, Equation 9 and Equation 10 were used to estimate the load-carrying capacity for the proposed model.

From the comparison presented in Table 10, the results from ABNT NBR 16935 (2021) [12] and Proposed Models differs for estimating the load-carrying capacity of the slabs tested by Alves et al. [25]. The ABNT NBR 16335 (2021) presented estimative over 1.5 times higher in comparison with the Proposed model.

This could be justified by the simplification of model proposed by ABNT NBR 16935 (2021) [12], where the tensile strength of the steel fiber reinforced concrete in the punching shear critical perimeter was $f_{R3}/3$. Silva [26] presented that the residual tensile strength of the steel fiber does not present a constant behavior in relation with the crack opening. This is also observed by other authors ([3], [4], [7], [8], [13]–[15], [22], and [23]). In additions, the use of safety factor for the steel fibers ($\gamma_F = 1{,}5$) still gives estimative higher than experimental tests.

The Proposed model recommend the use of a statistical parameter (k), which is based on experimental tests with similar conditions of the compressive behavior. The more experimental results used to calibrate the parameter k the better results for estimate the load-carrying capacity. From Table 3, for estimate the results of load-carrying capacity of Alves et al. [25] tests, the parameter k was calibrated with 23 experimental tests with similar compressive conditions (compressive strength in a range of 40-50 MPa, similar properties of steel fibers and similar content of steel fibers).

Although the results presented in Table 10 were in a good agreement with experimental test, the parameter k should be better calibrated for slabs reaching compressive strength of 60-90 MPa. A larger number of slabs is needed to improve the values of k in that range. However, Figure 5a presented that the estimative for the proposed model of all the 68 slabs data base were conservative results. In other words, in Figure 5a all the points representing the experimental tests were projected below the 1:1 line, where experimental load-carrying capacity is higher than the estimative from the proposed model.

5 CONCLUSIONS

This study presented a proposed model for estimate the punching shear load-carrying capacity for steel fiber reinforced concrete flat slabs. The proposed model was based on the Brazilian standard code by a logarithmic adjusted curve G for the contribution of steel fibers on punching. The adjusted function G was based on the results of 68 slabs experimental tests database.

For testing the accuracy of the load-carrying capacity estimate by the proposed model, the results were compared by the estimative of other authors steel fibers reinforced concrete punching shear models. The proposed model presents a better response in the analyzed slabs (mainly for load-carrying capacity up to 200kN) compared to the other analyzed models with an average of R_{em} of 1.3 and the highest confidence index of 96%, despite considering only the content of steel fiber as a parameter of fibers.

In relation to the R_{em}, average, the proposed equation has the same level of safety as the Brazilian standard equation, the Brazilian standard equation for slabs without fibers already has an experimental / theoretical load-carrying capacity ratio of 1.3, similar value found for the proposed model (both without safety factors).

In addition, a comparison with the ABNT 16935 (2021) [12] presented an estimative higher than the experimental results conducted by Alves et al. [25] where the proposed model presented a good agreement. This could be justified by the simplification on considering the residual tensile strength proposed by the ABNT NBR 16935 (2021) [12] while the proposed model is based on statistical parameter that could be improved incorporating more results from experimental tests.

The result of this paper is constantly in update with testing of parameters k and adjusted function G. The authors intend to incorporate other experimental tests in the database and analyze its sensibility to geometric and physical database parameters such as h, f_c, ρ, b_p, and V_f.

ACKNOWLEDGEMENTS

The authors would like to express their gratitude for the graduate program in civil engineering of the *Universidade Federal de Uberlandia* and the funding agency CAPES.

REFERENCES FORMATS

[1] D. A. Gasparini, "Contributions of C. A. P. Turner to Development of Reinforced Concrete Flat Slabs 1905–1909," *J. Struct. Eng.*, vol. 128, no. 10, pp. 1243–1252, 2002, http://dx.doi.org/10.1061/(ASCE)0733-9445(2002)128:10(1243).

[2] Associação Brasileira de Normas Técnicas, *Projetos de Estruturas de Concreto – Procedimento*, NBR 6118, 2014.

[3] L. G. Dantas, "Proposta para o cálculo de carga de ruptura por punção em lajes de concreto reforçado com fibras de aço," M.S. thesis, Univ. Fed. Uberlândia, Uberlândia, MG, Brasil, 2020. https://doi.org/10.14393/ufu.di.2020.374.

[4] R. Narayanan and I. Y. S. Darwish, "Punching shear tests on steel-fibre-reinforced micro-concrete slabs," *Mag. Concr. Res.*, vol. 39, no. 138, pp. 42–50, 1987, http://dx.doi.org/10.1680/macr.1987.39.138.42.

[5] J. A. O. Barros, B. N. Moraes Neto, G. S. S. A. Melo, and C. M. V. Frazão, "Assessment of the effectiveness of steel fibre reinforcement for the punching resistance of flat slabs by experimental research and design approach," *Compos., Part B Eng.*, vol. 8, no. 1, pp. 8–25, 2015, http://dx.doi.org/10.1016/j.compositesb.2015.03.050.

[6] V. S. S. Alves, "Avaliação do efeito de punção em lajes lisas de concreto com fibras com a variação do índice de retangularidade," M.S. thesis, Fac. Eng. Civ., Univ. Fed. Uberlândia, Uberlândia, MG, Brasil, 2017.

[7] A. Stanislav, N. Tošić and A. De La Fuente, "A limit state design approach for hybrid reinforced concrete column-supported flat slabs," *Struct. Concr.*, vol. 23, no. 6, pp. 3444–3464, 2022, http://dx.doi.org/10.1002/suco.202100785.

[8] L. H. B. Oliveira, "Resistência à punção em lajes lisas de concreto armado com adição de fibras de aço e aberturas adjacentes ao pilar," Ph.D. dissertation, Univ. Estad. Campinas, Fac. Eng. Civ., Arquit. Urb., Campinas, SP, Brasil, 2020.

[9] L. Facconi, F. Minelli, and G. Plizzari, "Steel fiber reinforced selfcompacting concrete thin slabs: experimental study and verification against model Code 2010 provisions," *Eng. Struct.*, vol. 122, pp. 226–237, 2016., http://dx.doi.org/10.1016/j.engstruct.2016.04.030.

[10] D. Fall, J. Shu, R. Rempling, K. Lundgren, and K. Zandi, "Two-way slabs: experimental investigation of load redistributions in steel fibre reinforced concrete," *Eng. Struct.*, vol. 80, pp. 61–74, 2014., http://dx.doi.org/10.1016/j.engstruct.2014.08.033.

[11] H. Higashiyama, A. Ota, and M. Mizukoshi, "Design equation for punching shear capacity of SFRC slabs," *Int. J. Concr. Struct. Mater.*, vol. 5, no. 1, pp. 35–42, Jun 2011.

[12] Associação Brasileira de Normas Técnicas, *Projetos de Estruturas de Concreto – Procedimento*, NBR 16935, 2021.

[13] D. D. Theodorakopoulos and N. Swamy, "Contribution of steel fibers to the strength characteristics of lightweight concrete slab-column connections falling in punching shear," *ACI Struct. J.*, vol. 90, no. 4, pp. 342–355, 1993, http://dx.doi.org/10.14359/3957.

[14] A. M. Shaaban and H. Gesund, "Punching shear strength of steel fiber reinforced concrete flat plates," *ACI Struct. J.*, vol. 91, no. 3, pp. 406–414, 1994, http://dx.doi.org/10.14359/4145.

[15] M. H. Harajli, D. Maalouf, and H. Khatib, "Effect of fibers on the punching shear strength of slab-column connections," *Cement Concr. Compos.*, vol. 17, no. 2, pp. 161–170, 1995, http://dx.doi.org/10.1016/0958-9465(94)00031-S.

[16] E. N. Z. Vargas, "Punção em lajes-cogumelo de concreto de alta resistência reforçado com fibras de aço. Dissertação, Esc. Eng. São Carlos, Univ. São Paulo, São Carlos, SP, Brasil, 1997.

[17] A. P. Azevedo, "Resistência e ductilidade das ligações laje-pilar em lajes-cogumelo de concreto de alta resistência armado com fibras de aço e armadura transversal de pinos," M.S. thesis, Eng. Estrut., Esc. Eng. São Carlos, Univ. São Paulo, São Carlos, SP, Brasil, 1999.

[18] P. J. McHarg, W. D. Cook, D. Mitchell, and Y. S. Yoon, "Benefits of concentrated slab reinforcement and steel fibers on performance of slab-column connections," *ACI Struct. J.*, vol. 97, no. 2, pp. 225–234, 2000, http://dx.doi.org/10.14359/851.

[19] T. H. Musse, "Punção em lajes cogumelos – fibras de aço e armadura de cisalhamento", M.S. thesis, Univ. Fed. Goiás, Goiânia, GO, Brasil, 2004.

[20] J. B. De Hanai and K. M. A. Holanda, "Similarities between punching and shear strength of steel fiber reinforced concrete (SFRC) slabs and beams," *Rev. IBRACON Estrut. Mater.*, vol. 1, no. 1, pp. 1–16, 2008.

[21] M. Y. Cheng and G. J. Parra-Montesinos, "Evaluation of steel fiber reinforcement for punching shear resistance in slab-column connections—Part I: monotonically increased load," *ACI Struct. J.*, vol. 107, no. 1, pp. 101–109, 2010, https://doi.org/10.14359/51663394

[22] L. Nguyen-Minh, M. Rovnak, and T. Tran-Quoc, "Punching shear capacity of interior SFRC Slab-Column connections," *J. Struct. Eng.*, vol. 138, no. 5, pp. 613–624, 2012, http://dx.doi.org/10.1061/(ASCE)ST.1943-541X.0000497.

[23] N. D. Gouveia, N. A. G. Fernandes, D. M. V. Faria, A. M. P. Ramos, and V. J. G. Lucio, "SFRC flat slabs punching behaviour – Experimental research," *Compos., Part B Eng.*, vol. 63, no. 1, pp. 161–171, 2014, http://dx.doi.org/10.1016/j.compositesb.2014.04.005.

[24] M. P. Collins, *Evaluation of shear design procedures for concrete structures. A Report prepared for the CSA technical committee on reinforced concrete design*, CSA, Canadian, 2001.

[25] V. Alves, L. Oliveira, A. Santos and L. Trautwein, Experimental evaluation of the load carrying capacity of SFRC flat slabs varying the rectangularity index of columns," *KSCE J. Civ. Eng.*, vol. 25, pp. 574–585, 2021.

[26] J. R. Silva, *Correlação de valores de tenacidade do concreto reforçado com fibras de aço obtidos pela ASTM C1609: 2012 E EN 14651: 2007*, M.S. thesis, Univ. Fed. Uberlândia, Uberlândia, MG, Brasil, 2018.

Author contributions: ACS and LMT: conceptualization, funding acquisition, supervision; LHBO and LGD: conceptualization, data curation, formal analysis, methodology, writing.

Editors: Ricardo Carrazedo, Guilherme Aris Parsekian.

IBRACON Structures and Materials Journal
Revista IBRACON de Estruturas e Materiais
ISSN 1983-4195 ismj.org

ERRATUM

Erratum: Proposal for estimating the punching shear load-carrying capacity of steel fibers reinforced concrete flat slabs

In the article **"Proposal for estimating the punching shear load-carrying capacity of steel fibers reinforced concrete flat slabs"**, DOI number https://doi.org/10.1590/S1983-41952023000500009, published in IBRACON Structures and Materials Journal ISSN 1983-4195, v.16, n.5, e16509, 2023, on page 11:

ACKNOWLEDGEMENTS

Where it reads:

The authors would like to express their gratitude for the graduate program in civil engineering of the *Universidade Federal de Uberlandia* and the funding agency CAPES.

It should be read:

The authors would like to express their gratitude for the graduate program in civil engineering of the *Universidade Federal de Uberlândia* and the funding agency *Fundação de Amparo à Pesquisa do Estado de Minas Gerais* (FAPEMIG) and *Coordenação de Aperfeiçoamento de Pessoal de Nível Superior* (CAPES).